Mass Transfer Effects in Emulsion Polymerization Systems. I. Diffusional Behavior of Chain Transfer Agents in the Emulsion Polymerization of Styrene

M. NOMURA,* H. SUZUKI, H. TOKUNAGA, and K. FUJITA

Department of Materials Science and Engineering, Fukui University, Fukui, Japan

SYNOPSIS

On the basis of the so-called two-films theory for mass transfer, a mathematical model for transfer of chain transfer agents from monomer droplets to polymer particles, where chain transfer agent molecules are consumed by the chain transfer reaction, is developed for an emulsion polymerization system. It is shown by the model that the concentration of chain transfer agent in the polymer particles during the polymerization is decreased to a value much less than that which would be attained if thermodynamic equilibrium for chain transfer agent were reached between the polymer particles and the monomer droplets, due mainly to the resistance to transfer of chain transfer agent molecules across the diffusion films at the interface between the monomer droplets and the water phase. The validity and utility of the model developed for predicting the diffusion and consumption rates for chain transfer agent are demonstrated experimentally using five normal aliphatic mercaptans from n-C_7 to n-C_{12} as chain transfer agents in the seeded emulsion polymerization of styrene. © 1994 John Wiley & Sons, Inc.

INTRODUCTION

It is well known that chain transfer agents (CTAs) such as mercaptans of high molecular weight are often used in emulsion polymerization systems to regulate the molecular weight of polymer produced. In some cases, other ingredients, which directly participate in the polymerization reaction, are also often used to modify the properties of latex produced. In these cases, the reacting species must be transported from one phase like monomer droplets, via the water phase, to monomer-swollen polymer particles where the reaction usually takes place. Therefore, it is important to clarify quantitatively the diffusional behavior of these reacting species in an emulsion polymerization system.

To date, only a few investigators[1-5] have discussed mass transfer problems in emulsion polymerization systems. Smith[1] showed experimentally that the consumption rate of mercaptan of sufficiently low molecular weight was the same in both emulsion and bulk polymerization systems, whereas, in the case of mercaptan of high molecular weight, the consumption rate of such mercaptan in an emulsion polymerization system was much lower than that observed in a bulk polymerization system, and that, in the emulsion polymerization of styrene, the apparent transfer constant of normal aliphatic mercaptans with carbon atoms less than 9 was practically constant, but began to decrease with an increase in the number of carbon atoms in mercaptan when it exceeded 10. This indicates that, in the case of mercaptan of high molecular weight, the mercaptan concentration in the polymer particles must become lower than that which would be attained if thermodynamic equilibrium for mercaptan were reached between the polymer particles and the monomer–mercaptan droplets because the rate of transport of mercaptan molecules is impeded by diffusion resistances located between the monomer droplets and the polymer particles.[2] Brooks[3,4] discussed the effect of mass transfer on emulsion polymerization and arrived at the conclusion that the interfacial resistance to mass transfer which took

* To whom correspondence should be addressed.

Journal of Applied Polymer Science, Vol. 51, 21–31 (1994)
© 1994 John Wiley & Sons, Inc. CCC 0021-8995/94/010021-11

place at the water–polymer particle boundary could have noticeable effects on the polymerization, although in most cases simple diffusion resistance would not affect the course of the polymerization. On the other hand, Harada et al.[5] have shown that, in the emulsion polymerization of styrene, mass transfer resistance at the interface between the monomer droplets and the water phase becomes dominant when the monomer droplets are large due to a low intensity of agitation.

In this paper, a mathematical model for the transport of CTA from monomer droplets to polymer particles, where CTA molecules are consumed by the chain transfer reaction, is first developed for emulsion polymerization systems on the basis of the so-called two-films theory for mass transfer.[6] Then, it will be demonstrated by the model that the concentration of CTA in the polymer particles during the polymerization can be decreased to a value much less than that which would be attained if thermodynamic equilibrium for CTA were reached between the polymer particles and the monomer droplets because of the resistance to mass transfer across the diffusion films at the interfaces between the monomer droplets and the water phase, and between the polymer particles and the water phase. Moreover, the model is extended so as to predict the consumption rate of CTA. The validity and utility of the model for predicting the diffusion and consumption rates of CTA will be demonstrated experimentally by using five normal aliphatic mercaptans from n-C_7 to n-C_{12} as CTA in the seeded emulsion polymerization of styrene.

A MATHEMATICAL MODEL FOR CTA TRANSPORT

The Concentration of CTA in the Polymer Particles

If we employ the classical two-films theory[6] to explain the mass transfer mechanism of CTA molecules among phases in an emulsion polymerization system, we have a schematic diagram of the concentration profile of CTA among phases as shown in Figure 1. The theory suggests that the two phases are in thermodynamic equilibrium at the interface, that there is consequently no resistance to transfer across the interface, and that the resistance to mass transfer occurs in the thin films on either side of the interface. At steady state, the rate of diffusion of CTA across each interface, J_T, is equal to the rate of consumption by chain transfer reaction in the polymer particles, r_T, and can be expressed, according to Figure 1, by the following diffusion equations, if the consumption of CTA in the water phase due to the reaction with the water-phase radicals is assumed to be negligible because the concentrations of both species in the water phase are extremely low:

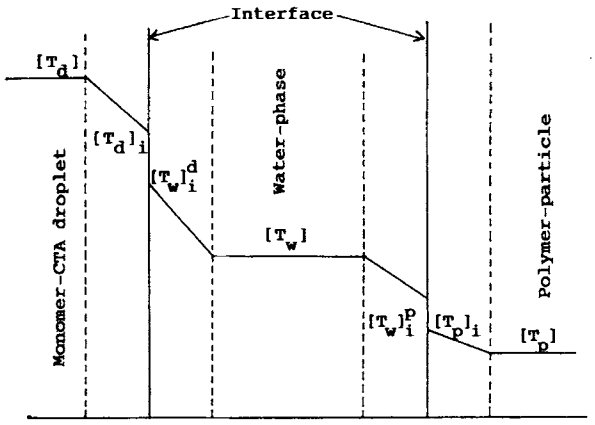

Figure 1 A schematic diagram of the concentration profile of chain transfer agent among phases.

$$J_T = k_{ld}A_d([T_d] - [T_d]_i) = k_{ldw}A_d([T_w]_i^d - [T_w])$$
$$= k_{lpw}A_p([T_w] - [T_w]_i^p) = k_{lp}A_p([T_p]_i - [T_p])$$
$$= k_T[T_p]\bar{n}N_p = r_T \qquad (1)$$

where k_{lk} is the film mass-transfer coefficient for a particular phase k, A_d and A_p are the surface areas of the monomer droplets and the polymer particles per cm^3 water, respectively, $[T_k]$ is the concentration of CTA in the bulk of the phase k, and $[T_k]_i^j$ is that in the phase k adjacent to the interface j. k_T is the rate constant for chain transfer to CTA, $\bar{n}$ is the average number of radicals per particle, N_p is the number of polymer particles per cm^3 water, and r_T is the consumption rate for CTA. The suffixes d, p, and w denote the monomer droplet, polymer particle, and water phases, respectively.

As stated above, we assume that the concentrations of CTA on either side of each interface are in thermodynamic equilibrium as shown below:

$$[T_d]_i = m[T_w]_i^d, \quad [T_p]_i = m'[T_w]_i^p \qquad (2)$$

where m and m' denote the partition coefficients of CTA.

Combining eqs. (1) and (2) and rearranging leads to the following expression which gives the overall resistance R for the transport of CTA from the monomer droplets to the polymer particles:

$$R = \frac{[T_d]}{r_T} = \left(\frac{1}{k_{ld}} + \frac{m}{k_{ldw}}\right)\frac{1}{A_d} + \left(\frac{m}{k_{lp}m'} + \frac{m}{k_{lpw}}\right)\frac{1}{A_p} + \frac{m}{k_T\bar{n}N_pm'} \quad (3)$$

The first and the second terms of the right-hand side of eq. (3) represent the diffusion resistances across the thin films at the interfaces between the monomer droplets and the water phase, and between the water phase and the polymer particles, respectively. The third term, on the other hand, denotes the so-called reaction resistance. Furthermore, it is evident from eq. (3) that we can evaluate the overall resistance R by measuring the concentration of CTA in the monomer droplets, $[T_d]$, and the consumption rate of CTA, r_r.

Let us consider the film mass transfer coefficient for CTA in the individual diffusion films. There are a large number of published studies concerning the film mass transfer coefficient in the outer diffusion film around a sphere in a flowing fluid. One of these is the following semitheoretical correlation proposed by Rantz and Marshall[7]:

$$Sh = k_l d/D = 2 + 0.6\, Sc^{1/3}\mathrm{Re}^{1/2} \quad (4)$$

where Sh is the Sherwood number, Sc is the Schmidt number $(\mu/\rho D)$, and Re is the Reynolds number $(du\rho/\mu)$. k_l is the film mass-transfer coefficient, d is the diameter of a sphere, D is the diffusion coefficient of CTA, u is the relative velocity between a sphere and a flowing fluid, μ is the viscosity in the diffusion film, and ρ is the density of the fluid. Since the monomer droplets and the polymer particles are so small, and the density difference between the spheres and the fluid is also so small, that these spheres will move with the eddies of the fluid in a stirred tank reactor for emulsion polymerization, there will be no relative velocity between the sphere and the fluid and accordingly, the value of Re can be regarded as zero, that is, $Sh = 2$. Then, we have

$$k_l = 2D/d \quad (5)$$

Considering that the values of m and m' are almost the same order of magnitude and are much larger than 10^3 as shown later, and that the film mass transfer coefficient in the inner diffusion film of a sphere is almost the same order of magnitude as that in the outer diffusion film given by eq. (5), eq. (3) can be approximated as

$$R = \frac{[T_d]}{r_T} = \left(\frac{m}{k_{ldw}}\right)\frac{1}{A_d} + \left(\frac{m}{k_{lpw}}\right)\frac{1}{A_p} + \frac{m}{k_T\bar{n}N_pm'} \quad (6)$$

The surface areas of monomer droplets and polymer particles per cm^3 water can be calculated by the following expressions:

$$A_d = \pi d_d^2 N_d, \quad A_p = \pi d_p^2 N_p \quad (7)$$

where d_d and d_p denote the average diameters of monomer droplets and polymer particles, respectively, and N_d and N_p are the numbers of monomer droplets and polymer particles per cm^3 water, respectively. Introducing eqs. (5) and (7) into eq. (6) leads to the final expression for the overall diffusion resistance

$$R = \frac{[T_d]}{r_T} = \frac{m}{2\pi D_T d_d N_d} + \frac{m}{2\pi D_T d_p N_p} + \frac{m}{k_T\bar{n}N_pm'} \quad (8)$$

where D_T is the diffusion coefficient of CTA in the water phase.

We can assume that the monomer concentration in the polymer particles is in thermodynamic equilibrium with that in the monomer droplets from the start to the end of polymerization because monomer molecules can transfer very rapidly among the phases, and further that the partition equilibrium of CTA between the polymer particles and the monomer particles is approximately the same as that for monomer.[8] Considering these and eq. (2), we can also assume the following simple linear partition equilibrium for CTA and monomer:

$$\frac{[T_p]_{eq}}{[T_d]} = \frac{[M_p]}{[M_d]} = \frac{m'}{m} \quad (9)$$

where $[T_p]_{eq}$ denotes the equilibrium concentration of CTA in the polymer particles which would be attained if there was no diffusion resistance to the transport of CTA from the monomer droplets to the polymer particles and thermodynamic equilibrium for CTA was reached between the monomer droplets and the polymer particles. $[M_p]$ and $[M_d]$ are the concentrations of monomer in the polymer particles and in the monomer droplets, respectively.

Using eqs. (8) and (9), we can derive the degree of saturation of CTA in the polymer particles, $[T_p]/[T_p]_{eq}$, which shows how far the actual concentra-

tion of CTA in the polymer particles is apart from the equilibrium concentration $[T_p]_{eq}$, owing to the diffusion resistance, as

$$\frac{[T_p]}{[T_p]_{eq}} = \frac{1}{1+\Omega},$$

$$\Omega = \frac{(m/2\pi D_T)(1/d_d N_d + 1/d_p N_p)}{m/k_T \bar{n} N_p m'} \quad (10)$$

A Model for Predicting the Consumption Rate for CTA

The conversion vs. time history for CTA can be predicted by using the mathematical model developed in the preceding section. The consumption rates for monomer and CTA are respectively expressed by the following well-known kinetic equations:

$$R_p = \frac{dX_M}{dt} = \frac{k_p[M_p]\bar{n}N_p M_m}{M_0 N_A} \quad (11)$$

$$R_T = \frac{dX_T}{dt} = \frac{k_T[T_p]\bar{n}N_p M_T}{T_0 N_A} \quad (12)$$

where k_p is the propagation rate constant, N_A is the Avogadoro's number, M_0 and T_0 are the weights of monomer and CTA initially charged per cm^3 water, X_M and X_T are the conversions of monomer and CTA, M_m and M_T are the molecular weights of monomer and CTA, respectively. In calculating the consumption rate of CTA by eq. (12), the experimental value of the average number of radicals per particle, $\bar{n}$, obtained by applying eq. (11) to the initial slope of the observed monomer conversion vs. time curve is used here. However, if it is necessary to predict the value of $\bar{n}$ theoretically, the following expression will be used[8]:

$$\bar{n} = \frac{1}{2}\left\{\left[\left(\alpha_w + \frac{\alpha_w}{m_w}\right)^2 + 2\left(\alpha_w + \frac{\alpha_w}{m_w}\right)\right]^{1/2} - \left(\alpha_w + \frac{\alpha_w}{m_w}\right)\right\} + \left(\frac{1}{4} + \frac{\alpha_w}{2}\right)^{1/2} - \frac{1}{2} \quad (13)$$

where the nondimensional parameters, α_w and m_w, are defined as $\alpha_w = (r_i v_p / k_{tp} N_p)$ and $m_w = (k_f v_p / k_{tp})$, respectively. Here, k_f denotes the rate coefficient for radical desorption from the polymer particles, k_{tp} is the rate constant for radical termination in the polymer particles, and r_i is the rate of radical production in the water phase.

Next, let us explain how to calculate the concentrations of monomer and CTA in both the polymer particles and the monomer droplets. Mass balances on monomer and CTA are written as

$$M_d + M_p = M_0(1 - X_M) \quad (14)$$

$$T_d + T_p = T_0(1 - X_T) \quad (15)$$

where M_d and M_p represent the weights of monomer contained in the polymer particles and in the monomer droplets per cm^3 water, respectively. T_0 is the weight of CTA initially charged per cm^3 water and T_d and T_p are the weights of CTA contained in the monomer droplets and in the polymer particles, respectively. The total volumes of polymer particles, V_p, and monomer droplets, V_d, per cm^3 water and their individual volumes, v_p and v_d, can be expressed approximately by the following equations, respectively:

$$V_p = v_p N_p = \left(\frac{M_p}{\rho_m}\right) + \left(\frac{T_p}{\rho_T}\right) + \left(\frac{M_0 X_M}{\rho_p}\right) \quad (16)$$

$$V_d = v_d N_d = \left(\frac{M_d}{\rho_m}\right) + \left(\frac{T_d}{\rho_T}\right) \quad (17)$$

where ρ_m, ρ_p, and ρ_T are the densities of monomer, its polymer, and CTA, respectively. The concentrations of monomer and CTA in both the polymer particles and the monomer droplets, on the other hand, can be calculated in mol/dm^3 by the following respective equations derived with the assumption that the volume of each component (monomer, polymer and CTA) is additive:

$$[M_p] = \frac{10^3 M_p}{M_m V_p} \quad (18)$$

$$[M_d] = \frac{10^3 M_d}{M_m V_d} \quad (19)$$

$$[T_p] = \frac{10^3 T_p}{M_T V_p} \quad (20)$$

$$[T_d] = \frac{10^3 T_d}{M_T V_d} \quad (21)$$

Furthermore, we can derive the following equation which connects $[T_p]$ with $[T_d]$, from eqs. (9) and (10):

$$\frac{[T_p]}{[T_d]} = \frac{(m'/m)}{1+\Omega} \quad (22)$$

where Ω denotes the ratio of the total diffusion resistance to the so-called reaction resistance in the polymer particles defined by eq. (10).

EXPERIMENTAL

Materials

Styrene monomer of commercial grade was washed with 15% aqueous KOH solution to remove inhibitor. The monomer thus treated was further washed with deionized water, then distilled twice under reduced nitrogen pressure, and stored at −20°C in a refrigerator. Five commercially available normal aliphatic mercaptans (n-C_7, n-C_8, n-C_9, n-C_{10}, and n-C_{12}) of reagent grade were used without further purification. Potassium persulfate (KPS) and sodium laurylsulfate (NaLS) of extra pure grade were used as received as initiator and emulsifier, respectively. Deionized and distilled water was used in all experiments. The diameter of polystyrene seed latexes used in these experiments was 35 nm. These polystyrene seed latexes were prepared by synthesizing at 70°C using the same reactor, initiator, and emulsifier. The polymerization for preparation of seed latex was completed until nearly no residual monomer could be detected. A portion of the latex thus produced (80 cm^3) was then washed with about 500 cm^3 of 0.05% NaLS aqueous solution through a Millipore membrane filter with a nominal molecular weight limit of 10^4 in a ultrafiltration apparatus to remove the residual initiator in the aqueous phase of the seed latex. The polystyrene seed latex thus prepared was stored at 5°C in a refrigerator just before use.

Apparatus and Experimental Procedure

Emulsion polymerization experiments were carried out in a cylindrical glass reactor of 75 mm diameter (400 cm^3) with a dished bottom, equipped with a four-blade paddle-type impeller. Four baffles made of stainless steel were set on the reactor wall at every 90° interval to improve mixing of the reaction mixture. The dimensions of the reactor, buffles, and impeller are the same as those used in the previous experiments.[5] The reactor was first charged with the desired amounts of monomer, chain transfer agent, emulsifier, and purified water, a small portion of which was put aside for preparing an aqueous initiator solution. A small amount of NaLS emulsifier was added to the reaction mixture so as to be 0.3 g/dm^3 water to avoid coagulation of polymer particles. The desired amount of mercaptan was charged as a monomer solution so that the initial concentration of mercaptan was 4.22×10^{-5} mol/g monomer in all experiments. Then, the dissolved oxygen was purged by bubbling pure nitrogen gas (99.995%) through the reaction mixture for about 20 min. The polymerization was started by pouring the aqueous initiator solution, which had been deoxygenated with the pure nitrogen gas and stored in a dropping funnel, into the reaction mixture. In all experiments, the reaction temperature was kept within 50 ± 0.5°C in a thermostatted water bath. Impeller speed was 400 rpm unless otherwise stated. Monomer conversion was determined gravimetrically and mercaptan conversion was measured by gas chromatography (GC) with a flame photometric detector (FPD). Samples for the measurement of monomer and mercaptan conversions were withdrawn from the sampling cock attached to the bottom of the reactor. Polymer was precipitated by pouring the weighed sample into excess acidified methanol, collected by filtration with a G4 glass crucible, dried overnight at 50°C in an oven, and weighed for determination of monomer conversion. The filtrate was, on the other hand, subjected to GC measurement for determination of mercaptan conversion.

RESULTS AND DISCUSSION

Figure 2 shows typical examples of the mercaptan conversion vs. time curves observed when the number of carbon atoms in normal aliphatic mercaptan was changed from 7 to 12 with the number of seed polymer particles, the initial initiator, monomer, and mercaptan concentrations fixed at constant. The solid line through the closed circles shows the conversion vs. time curve for styrene monomer. It is seen that the initial regions of the conversion vs. time curves for each mercaptan and the monomer are almost linear and that the rate of mercaptan consumption decreases drastically with increasing the number of carbon atoms in mercaptan, although the value of the chain transfer constant for each mercaptan is almost the same.

Next, let us explain how to calculate the observed initial value of $[T_p]/[T_p]_{eq}$. The initial concentration of mercaptan in the polymer particles, $[T_p]_0$, can be obtained by introducing both the initial consumption rates for mercaptan, R_{T0}, and for monomer, R_{p0}, determined from the initial slope of respective conversion vs. time curves, to the following expression which was derived from eqs. (11) and (12):

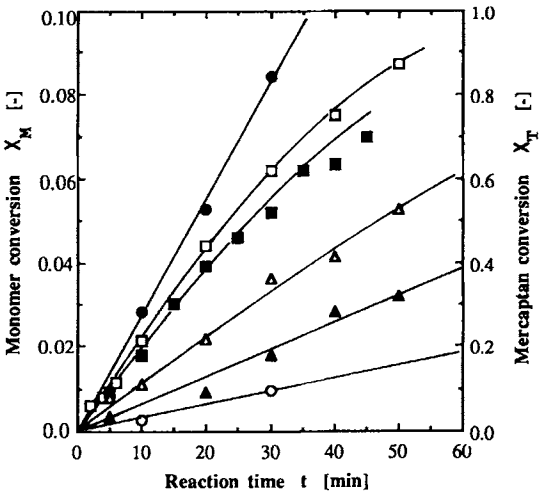

Figure 2 Typical examples of the mercaptan conversion vs. time curves observed when the number of carbon atoms in mercaptan is changed. Recipe and reaction conditions: 50°C, M_0 = 0.2 g/cm^3 water, I_0 = 1.25 g/dm^3 water, S_0 = 0.3 g/dm^3 water, $N_p = 1.0 \times 10^{14}$ particles/cm^3 water, $d_{p0} = 4.8 \times 10^{-6}$ cm, $T_{m0} = 8.44 \times 10^{-6}$ mol/cm^3 water. (●) Monomer conversion; Mercaptan conversion: (□) n-C_7; (■) n-C_8; (△) n-C_9; (▲) n-C_{10}; (○) n-C_{12}.

$$[T_p] = \left(\frac{T_0 M_m}{M_0 M_T}\right)\left(\frac{R_T}{R_p}\right)\left(\frac{[M_p]}{C_T}\right) \qquad (23)$$

where C_T denotes the chain transfer constant to mercaptan, k_T/k_p. Furthermore, the initial mercaptan concentration in the monomer droplets, $[T_d]_0$, can be calculated by the following mass balance on the mercaptan initially charged:

$$[T_p]_0 V_{p0} + [T_d]_0 V_{d0} = T_{m0} \qquad (24)$$

where V_{p0} and V_{d0} are the initial volumes of the monomer-swollen seed polymer particles and the monomer–mercaptan droplets per cm^3 water, respectively. T_{m0} is the number of moles of mercaptan initially charged per cm^3 water. Assuming that the volume of each component in the polymer particles is additive, and further that the initial volume of mercaptan absorbed by the monomer-swollen seed polymer particles is negligible because the weight of seed polymer particles initially charged is very small, we can calculate the volume V_{p0} by

$$V_{p0} = \left(\frac{\gamma}{\rho_m} + \frac{1}{\rho_p}\right) P_0 \qquad (25)$$

where P_0 is the weight of seed polymer particles initially charged per cm^3 water, ρ_p is the density of polymer, and γ is the so-called monomer/polymer ratio (M/P). The first term of the right-hand side of eq. (25) denotes the volume of monomer absorbed by the seed polymer particles, so that the volume of monomer droplets, V_{d0}, can be calculated by subtracting the volume of monomer absorbed by the seed polymer particles, $\gamma P_0/\rho_m$, from the volume of monomer initially charged, V_0. All the numerical constants used in this work are listed in Table I except for the values of m and D_T, which will be shown later in Table II.

Table I Numerical Values of the Parameters Used (50°C)

Constant	Value	Unit
k_p[13]	212	dm^3/mol sec
C_T	20	—
m'/m	0.65	—
d_{p0}	35	nm
ρ_m	0.88	g/cm^3
ρ_p	1.05	g/cm^3
ρ_T	0.83	g/cm^3
γ[13]	0.33	—
$k_d f$[13]	6.7×10^{-7}	1/s

The observed initial value of $[T_p]/[T_p]_{eq}$ for each mercaptan, calculated by applying eqs. (9) and (23)–(25) to the experimental data in Figure 2, is presented in Figure 3 to compare with the theoretical prediction. The theoretical values of $[T_p]/[T_p]_{eq}$ shown by the solid lines in Figure 3 were calculated by eq. (10) with changing initial diameter of monomer droplets, d_{d0}, and the value of the partition coefficient of mercaptan, m. The value of $\bar{n}$ used in these calculation was 0.5. The values of m and D_T for each mercaptan are listed in Table II. The value of D_T was predicted by the semiempirical correlation given by Wilke and Chang.[9] The values of m for n-C_7, n-C_8, and n-C_9 mercaptans were calculated directly

Table II Partition Coefficients and Diffusion Coefficients for Normal Aliphatic Mercaptans Used

Mercaptan	m [—]	D_T (cm/s)
n-C_7	6.0×10^4	8.0×10^{-6}
n-C_8	2.1×10^5	7.5×10^{-6}
n-C_9	7.0×10^5	7.0×10^{-6}
n-C_{10}	2.5×10^6	6.6×10^{-6}
n-C_{12}	4.9×10^7	6.0×10^{-6}

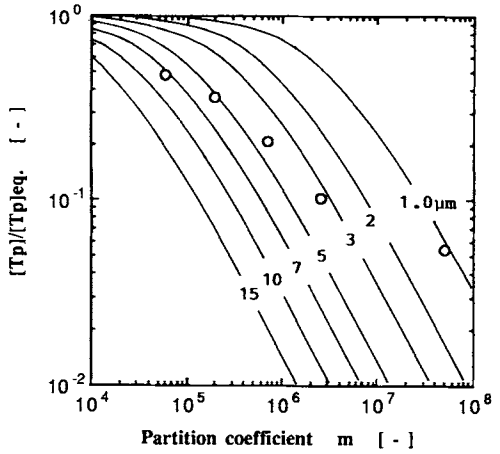

Figure 3 Comparison between the observed and calculated results: Effect of partition coefficient of mercaptan, m, on the initial value of the degree of saturation of mercaptan in the polymer particles, $[T_p]/[T_p]_{eq}$ (data correspond to those in Fig. 2).

from the water-solubility data at 25°C shown in Figure 4.[10] On the other hand, the values of m for n-C_{10} and n-C_{12} mercaptans, whose solubility data are not given in Figure 4, were calculated by using the estimated values obtained by extrapolation in the figure. Although the value of D_T changes slightly with the number of carbon atoms in mercaptan, the value of $D_T = 7.0 \times 10^{-6}$ cm/s was used as an average value in these calculations. It is seen in Figure 3 that most experimental data points gather around the theoretical lines for d_{d0} = 3–7 μm except the data point for n-C_{12}. This means that when impeller speed was 400 rpm, the initial average diameter of monomer droplets must be within 5 ± 2 μm, which agrees well with the recent experimental data reported in the presence of a surface-active agent,[11] and also with our experimental finding obtained in a reactor with almost the same dimensions and conditions as adopted in these experiments.[12] Only the data point for n-C_{12} mercaptan deviates far from these theoretical lines and is rather close to the theoretical line for d_{d0} = 1.0 μm. It is very doubtful that the initial average diameter of monomer droplets, d_{d0}, is around 1 μm only in the system with n-C_{12} mercaptan, although we did not measure it. The reason for this is not clear because we could not succeed in measuring the exact value for the water solubility of n-C_{12} mercaptan due to its great difficulty, but may be rather that the estimated water solubility of n-C_{12} mercaptan is lower by about an order of magnitude than the actual value.

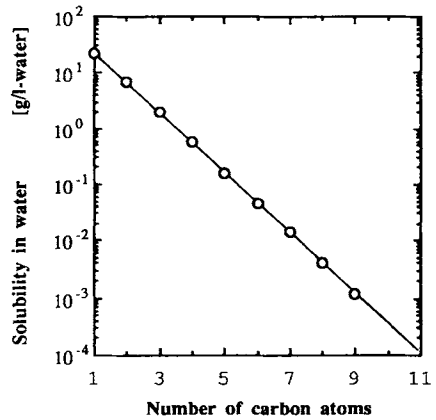

Figure 4 Literature data for the solubility of normal aliphatic mercaptan in water at 25°C vs. the number of carbon atoms in the mercaptan.

Furthermore, the effects of the number of seed polymer particles, N_p, and the amount of monomer, M_0, initially charged per cm³ water on the initial value of $[T_p]/[T_p]_{eq}$ were investigated by using n-C_{12} mercaptan. The experimental values are plotted with open circles in Figures 5 and 6, respectively, to compare with the theoretical predictions obtained by eq. (10) with $\bar{n} = 0.5$. The closed circles in these figures represent the values to which the experimental values were corrected according to eq. (10) so as to correspond to $\bar{n} = 0.5$. It is seen that all the corrected data points in these figures fall on the theoretical line close to that for d_{d0} = 1.0 μm, as can be expected from the data point for n-C_{12} mercaptan

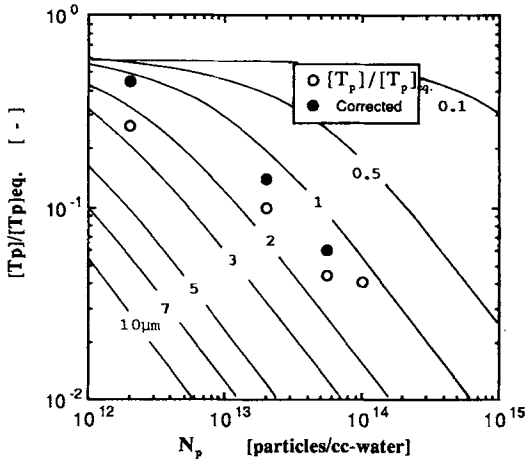

Figure 5 Comparison between the observed and calculated results: Effect of the number of seed polymer particles, N_p, initially charged on the initial value of the degree of saturation of n-C_{12} mercaptan in the polymer particles, $[T_p]/[T_p]_{eq}$. Recipe and reaction conditions: same as those in Figure 2 except for $N_p = 2.0 \times 10^{12}$, 2.0×10^{13}, 5.5×10^{13}, 1.0×10^{14} particles/cm³ water.

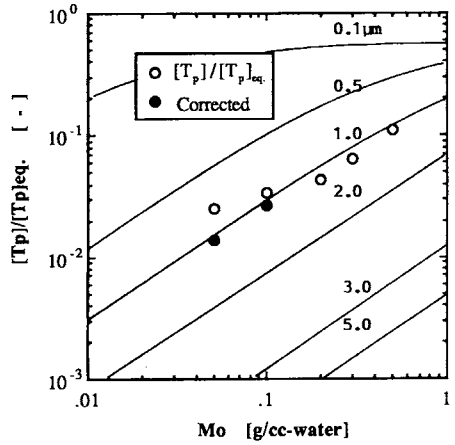

Figure 6 Comparison between the observed and calculated results: Effect of the initial monomer concentration M_0 on the initial value of the degree of saturation of n-C_{12} mercaptan in the polymer particles, $[T_p]/[T_p]_{eq}$. Recipe and reaction conditions: same as those in Figure 2 except for the initial monomer concentration; M_0 = 0.05, 0.10, 0.20, 0.30, 0.50 g/cm^3 water.

shown in Figure 3, although d_{d0} = 1.0 μm may be doubtful due to the reason mentioned previously.

In Table III, on the other hand, several examples are represented where the percent resistance (the ratio of each resistance to the overall diffusion resistance), which was calculated according to eq. (8), are compared when the kind of mercaptans and the reaction conditions are changed, to make clear which resistance is the most significant among three resistances. These are the diffusion resistance across the thin films at the interface between the monomer droplets and the water phase, the diffusion resistance across the thin films at the interface between the water phase and the polymer particles, and the so-called reaction resistance in the polymer particles. Here, R_d denotes the percent resistance for the diffusion step across the interfacial diffusion films around the monomer droplets, R_p is that for the diffusion step across the interfacial diffusion films around the polymer particles, and R_r shows that for the so-called reaction resistance. From the comparison shown in the table, we can consider that, in the case where C_{12} mercaptan is used and $N_p > 1 \times 10^{14}$ particles/cm^3 water, the principal diffusion resistance for the mercaptan is located in the mass transfer step from the monomer droplets to the water phase.

It is concluded from the comparisons shown above that the analysis of mass transfer resistance by the present model gives reasonable results except for the doubtful prediction that the average diameter of monomer droplets in the presence of n-C_{12} mercaptan is around 1 μm. It is also concluded that when the values of m for transporting species are less than 10^4, the diffusion resistances for them can be practically neglected in emulsion polymerization systems.

Next, let us examine whether the mathematical model developed in this work can predict the mercaptan conversion versus time history, (1) by assuming that the number of monomer droplets, N_d, remains constant throughout the polymerization, or (2) by assuming that the average diameter of monomer droplets, d_d, remains constant during the entire course of the polymerization. In Figure 7(a), an example of comparison between the calculated and experimental conversion vs. time data for n-C_{12} mercaptan is presented to see which of the above assumptions is much closer to the actual situation. The dotted line is the calculated conversion vs. time history for n-C_{12} mercaptan obtained with the former assumption that the number of monomer droplets is constant at $N_d = N_{d0} = 1.1 \times 10^{12}$ droplets/cm^3 water, which corresponds to the initial diameter of the monomer–mercaptan droplets, d_{d0} = 1.0 μm, while the solid line through the closed circles is that calculated with the latter assumption that the average diameter of the monomer droplets is constant at d_{d0} = 1.0 μm as long as the monomer–mercaptan droplets exist in the water phase. The solid line through the open circles, on the other hand,

Table III Comparison of % Resistances for the Respective Diffusion and Reaction Steps in Transport of Mercaptan Molecules from Monomer Droplets to Polymer Particles[a]

	M_0	N_p	d_p	d_d	R	R_d (%)	R_p (%)	R_r (%)	m
n-C_7	0.2	1.0×10^{14}	0.1	7	3.3×10^3	47	0	53	6.0×10^4
n-C_{12}	0.5	1.0×10^{14}	0.1	1	1.3×10^4	79	8	13	
	0.2	2.0×10^{13}	0.1	1	4.0×10^4	64	14	22	2.9×10^4
	0.2	1.0×10^{14}	0.1	1	2.9×10^4	90	4	6	

[a] Units: M_0 = g/cm^3 water, d_p = μm, d_d = μm, R = s.

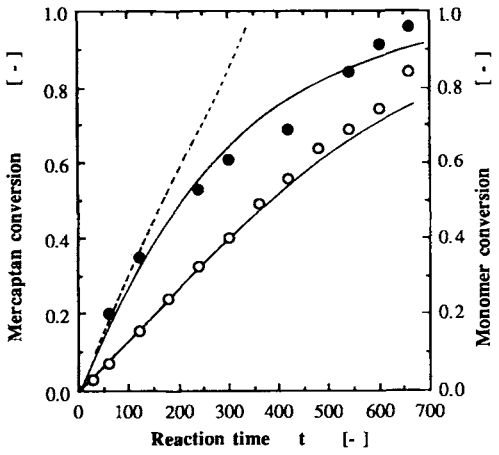

Figure 7 (a) Comparison between the calculated and observed conversion vs. time data for n-C_{12} mercaptan. Recipe and reaction conditions: same as those in Figure 2 except for M_0 = 0.5 g/cm^3 water. Experimental: (○) monomer conversion; (●) n-C_{12} mercaptan conversion. Calculation: (——) $d_d = d_{d0}$ = 1.0 μm); (· · ·) $N_d = N_{d0}$ = 1.1 × 10^{12}/cm^3 water.

shows the monomer conversion vs. time curve calculated with $\bar{n}$ = 0.55. Considering that the experimental data points given by the closed circles agree much better with the solid line than with the dotted line, we can conclude that the latter assumption (2) is much closer to the actual situation compared with the former assumption (1). Figure 7(b) plots the calculated monomer and mercaptan concentrations in the polymer particles vs. monomer conversion. Figure 7(c) shows the calculated variation of the number, N_d, and the total volume, V_d, of the monomer–mercaptan droplets per cm^3 water with the monomer conversion, corresponding to Figure 7(a). As can be seen from Figure 7(b), the present model predicts that the monomer concentration in the polymer particles is 5.45 mol/dm^3 particles up to around 40% monomer conversion and then decreases almost linearly with the monomer conversion, which coincides very well with the experimental observation so far obtained in the emulsion polymerization of styrene,[12] while the mercaptan concentration in the polymer particles decreases gradually with the monomer conversion from about 2.8 mol/dm^3 particles without any drastic change even in the vicinity of 40% monomer conversion, where the monomer-mercaptan droplets have almost depleted, as can be seen from Figure 7(c).

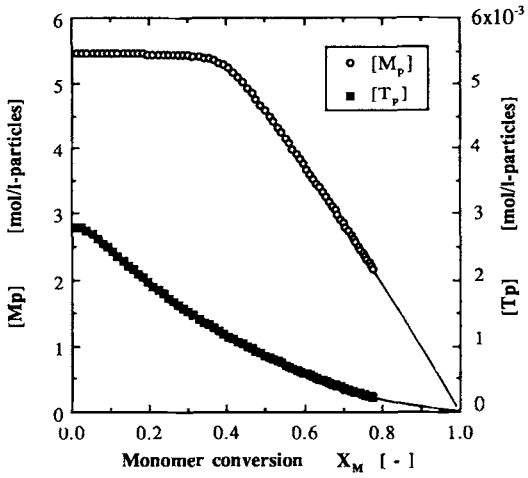

Figure 7 (b) Calculated variation of the concentrations of monomer and mercaptan in the polymer particles with the monomer conversion corresponding to Figure 7(a).

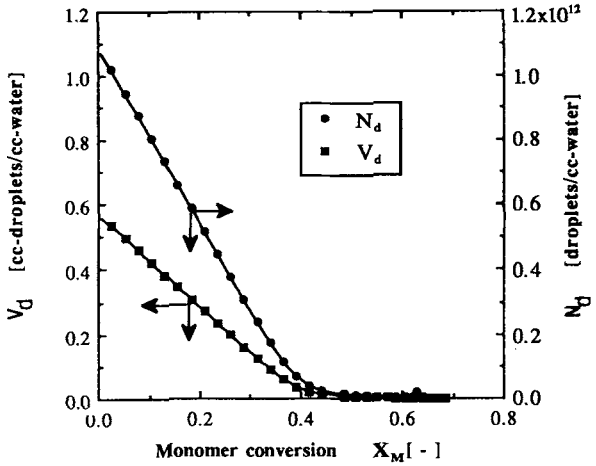

Figure 7 (c) Calculated variation of the number and the total volume of monomer–mercaptan droplets per cm^3 water with the monomer conversion corresponding to Figure 7(a).

In order to examine in more detail whether the assumption (2) can really be satisfied during the whole course of the polymerization, even when the reaction conditions such as M_0, N_p, and m are widely changed, comparisons were carried out between the experimental and predicted conversion vs. time histories by changing the values of M_0, N_p, and m (the kind of mercaptan). A few examples of the comparison are represented in Figures 8, 9, and 10, respectively. The closed circles in these figures show the experimental conversion vs. time data for mercaptans, while the solid lines are the theoretical conversion vs. time curves for them predicted by using eqs. (10)–(22). The open circles in Figures 9 and 10, on the other hand, denote the experimental monomer conversion vs. time data, and the solid lines through these data points show the predicted

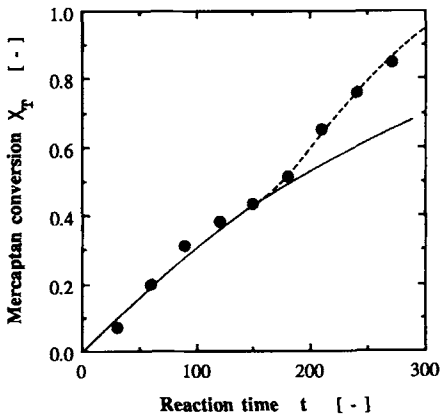

Figure 8 (a) Comparison between the calculated and observed conversion vs. time data for n-C_{12} mercaptan. Recipe and reaction conditions: same as those in Figure 2. Calculation: (——) $d_d = d_{d0} = 1.0$ μm when $0 \leq X_M \leq 1.0$; (· · ·) $d_d = d_{d0} = 1.0$ μm when $X_M < 0.44$, and $N_d = N_{d0} = 1.84 \times 10^{10}$/cm^3 water when $X_M \geq 0.44$.

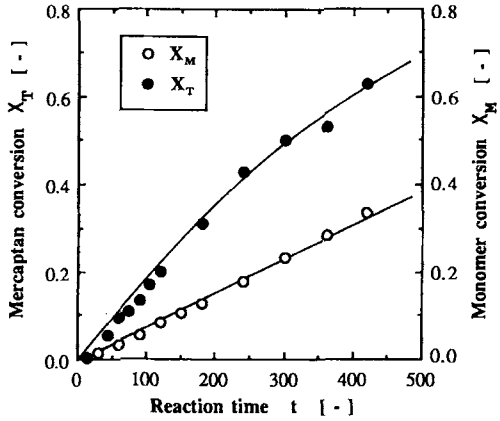

Figure 9 Comparison between the calculated and observed conversion vs. time data for n-C_{12} mercaptan. Recipe and reaction conditions: same as those in Figure 8(a) except for $N_p = 2.0 \times 10^{13}$ particles/cm^3 water.

monomer conversion vs. time curves calculated by using eqs. (10)–(22). Figure 8(a) shows a comparison between the predicted and observed conversion versus time history for n-C_{12} mercaptan when only the initial monomer concentration, M_0, was changed from 0.5 to 0.2 g/cm^3 water. Theoretical calculations were carried out with the experimental value of $\bar{n} = 0.5$ and $d_{d0} = 1.0$ μm. It is seen that the observed consumption rate of the mercaptan is in good agreement with the predicted one up to about 50% conversion, but suddenly accelerates around this conversion and begins to deviate from the predicted values. A slight indication of the same tendency could also be seen in the higher conversion range in the case of $M_0 = 0.5$ g/cm^3 water shown in Figure 7(a). The reason for this seems to be that, in the region where $X_M \geq 0.44$, the number of monomer–mercaptan droplets becomes higher than that predicted with the assumption that the average diameter of the monomer–mercaptan droplets remains constant. In order to check whether this is the case or not, the observed data are compared in Figure 8(a) with the predicted values shown by the dotted line, which was calculated by assuming that in the region where $X_M \geq 0.44$, the number of monomer–mercaptan droplets, N_d is kept constant at the value determined at $X_M = 0.44$ (1.84×10^{10} droplets/cm^3 water). Considering that the calculated line is in

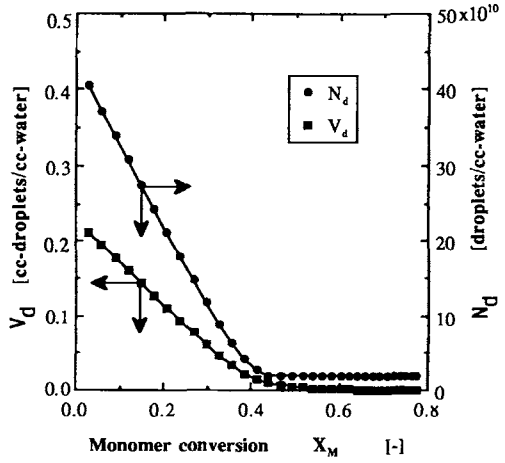

Figure 8 (b) Calculated variation of the number and the total volume of monomer–mercaptan droplets per cm^3 water with the monomer conversion corresponding to Figure 8(a).

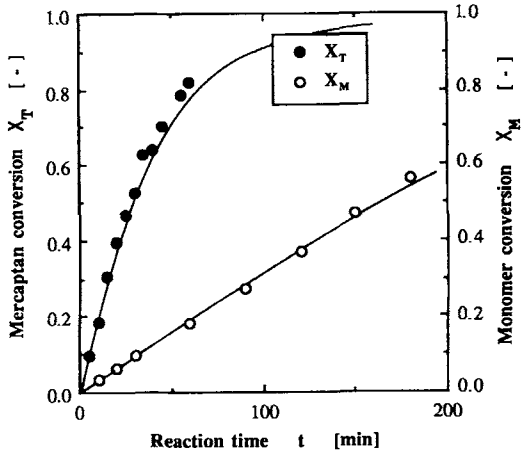

Figure 10 Comparison between the calculated and observed conversion vs. time data for n-C_8 mercaptan. Recipe and reaction conditions: same as those in Figure 2.

good agreement with the observed data points, we can conclude that in the region where $X_M \geq 0.44$, the number of the monomer–mercaptan droplets is kept rather constant at the value determined at $X_M = 0.44$, as is expected, although the average diameter of the monomer–mercaptan droplets remains approximately constant in the region where $X_M < 0.44$. This means that the coalescence rate of the monomer–mercaptan droplets would be greatly decreased or practically zero in the region where $X_M \geq 0.44$. This could take place, considering that the total volume of the monomer–mercaptan droplets was so low in this region, as shown in Figure 8(b) (e.g., $V_d = 0.0096$ cm^3/cm^3 water at $X_M = 44\%$ and $X_T = 43.5\%$), where the calculated variations of the number and total volume of the monomer–mercaptan droplets per cm^3 water with monomer conversion are shown. The predicted and observed conversion versus time histories for the monomer and n-C_{12} mercaptan are compared in Figure 9, where only the number of seed polymer particles initially charged was decreased to 2.0×10^{13} particles/cm^3 water. Theoretical calculations were carried out with the experimental value of $\bar{n} = 0.66$ and $d_{d0} = 1.2$ μm. Fairly good agreement can be seen, although a somewhat higher value for the average diameter of monomer–mercaptan droplets was necessary compared with other cases with n-C_{12} mercaptan. Figure 10, on the other hand, shows comparisons between the predicted and observed conversion vs. time curves for both the monomer and n-C_8 mercaptan. The calculated lines obtained using the experimental value of $\bar{n} = 0.5$ and $d_{d0} = 4.0$ μm agree very well with the experimental data points. We can conclude from the comparisons shown in Figures 7–10 that the present model can also give a good prediction for the consumption rate of CTA with the assumption that the average diameter of the monomer–CTA droplets remains approximately constant in the region where $X_M < 0.44$, while, in the region where $X_M \geq 0.44$, the number of these droplets is kept rather constant at the value determined at $X_M = 0.44$.

CONCLUSION

It was experimentally demonstrated that the concentration of CTA in the polymer particles during the course of polymerization could be decreased to a value much less than that which would be attained if thermodynamic equilibrium for CTA was reached between the polymer particles and the monomer droplets. We developed a mathematical model to explain this experimental finding quantitatively and demonstrated theoretically that the decrease in the concentration of CTA in the polymer particles was due mainly to the resistance to mass transfer across the diffusion films at the interfaces between the monomer droplets and the water phase. It was also demonstrated that the proposed model could predict well the consumption rate for CTA in the polymer particles with the assumption that the average diameter of the monomer–CTA droplets remains rather constant in the region where $X_M < 0.44$, while, in the region where $X_M \geq 0.44$, the number of these droplets is kept approximately constant at the value determined at $X_M = 0.44$.

It is supposed that the proposed model can also be applicable to the transport of any sparingly water-soluble reacting species from the monomer droplets to the polymer particles where these molecules participate in reactions.

REFERENCES

1. W. V. Smith, *J. Am. Chem. Soc.*, **68,** 2064 (1946).
2. F. A. Bovey, I. M. Kolthoff, A. I. Medalia, and E. J. Meehan, Eds., *Emulsion Polymerization,* Chap. IV, Wiley-Interscience, New York, 1955.
3. B. W. Brooks, *Br. Polym. J.*, **2,** 197 (1970).
4. B. W. Brooks, *Br. Polym. J.*, **3,** 269 (1971).
5. M. Harada, M. Nomura, H. Kojima, W. Eguchi, and S. Nagata, *J. Appl. Polym. Sci.*, **16,** 811 (1972).
6. W. K. Lewis and W. G. Whitman, *Ind. Eng. Chem.*, **16,** 1215 (1924).
7. W. E. Rantz and W. R. Marshall, Jr., *Chem. Eng. Progr.*, **48,** 141 (1952).
8. M. Nomura and K. Fujita, *Makromol. Chem., Suppl.* **10/11,** 25 (1985).
9. C. R. Wilke and P. C. Chang, *AlChEJ.*, **1,** 264 (1955).
10. The Chemical Society, Japan, Ed., *Kagaku Binran, Oyohen,* 1973, p. 801.
11. M. Konno, N. Kosaka, and S. Saito, *J. Chem. Eng. Jpn.*, **26,** 37 (1993).
12. M. Nomura, M. Harada, W. Eguchi, and S. Nagata, *J. Appl. Polym. Sci.*, **16,** 835 (1972).

Received April 9, 1993
Accepted May 18, 1993